ARMY RESEARCH LABORATORY

Exploratory Corrugated Infrared Hot-Electron Transistor Arrays

by Kwong-Kit Choi, Richard Fu, and Kimberly Olver

ARL-TR-4732 **February 2009**

NOTICES

Disclaimers

The findings in this report are not to be construed as an official Department of the Army position unless so designated by other authorized documents.

Citation of manufacturer's or trade names does not constitute an official endorsement or approval of the use thereof.

Destroy this report when it is no longer needed. Do not return it to the originator.

Army Research Laboratory
Adelphi, MD 20783-1197

ARL-TR-4732 **February 2009**

Exploratory Corrugated Infrared Hot-Electron Transistor Arrays

Kwong-Kit Choi, Richard Fu, and Kimberly Olver
Sensors and Electron Devices Directorate, ARL

REPORT DOCUMENTATION PAGE			Form Approved OMB No. 0704-0188

1. REPORT DATE *(DD-MM-YYYY)*	2. REPORT TYPE	3. DATES COVERED (From - To)
February 2009	Final	

4. TITLE AND SUBTITLE	5a. CONTRACT NUMBER
Exploratory Corrugated Infrared Hot-Electron Transistor Arrays	5b. GRANT NUMBER
	5c. PROGRAM ELEMENT NUMBER

6. AUTHOR(S)	5d. PROJECT NUMBER
Kwong-Kit Choi, Richard Fu, and Kimberly Olver	5e. TASK NUMBER
	5f. WORK UNIT NUMBER

7. PERFORMING ORGANIZATION NAME(S) AND ADDRESS(ES)	8. PERFORMING ORGANIZATION REPORT NUMBER
U.S. Army Research Laboratory ATTN: AMSRD-ARL-SE-EI 2800 Powder Mill Road Adelphi MD 20783-1197	ARL-TR-4732

9. SPONSORING/MONITORING AGENCY NAME(S) AND ADDRESS(ES)	10. SPONSOR/MONITOR'S ACRONYM(S)
	11. SPONSOR/MONITOR'S REPORT NUMBER(S)

12. DISTRIBUTION/AVAILABILITY STATEMENT

Approved for public release; distribution unlimited.

13. SUPPLEMENTARY NOTES

14. ABSTRACT

In this study, we investigated a 5×8 corrugated infrared hot-electron transistor (IHET) array with a common base configuration. We found the IHET structure improved the photocurrent-to-dark current ratio by a maximum factor of six compared to the basic quantum well infrared photodetector (QWIP) structure. This improvement is consistent with the hot-electron distributions created by the thermal and photo-excitations within the detectors. The study also showed that there is no electrical cross-talk among individual detectors, even though they share the same emitter and base contacts. Thus, the IHET structure is compatible with existing electronic readout circuits for photoconductors in producing sensitive focal plane arrays. Though not essential in this study, the apparent barrier height of the filter in the present material was higher than the designed value. This higher barrier height can be attributed to the finite p-type doping density in the material.

15. SUBJECT TERMS

QWIP, transistor, infrared

16. SECURITY CLASSIFICATION OF:			17. LIMITATION OF ABSTRACT	18. NUMBER OF PAGES	19a. NAME OF RESPONSIBLE PERSON
a. REPORT	b. ABSTRACT	c. THIS PAGE			Kwong-Kit Choi
U	U	U	UU	18	19b. TELEPHONE NUMBER (*Include area code*) (301) 394-0495

Standard Form 298 (Rev. 8/98)
Prescribed by ANSI Std. Z39.18

Contents

List of Figures

1. Objective

The objective of this work is to demonstrate an advanced quantum well infrared photodetector (QWIP) sensor in a small exploratory array format, which is capable of suppressing the detector dark current. The new detector is known as the infrared hot-electron transistor (IHET) (*1*). An IHET is a QWIP with a built-in electron energy filter and contains three terminals. The QWIP is located between the emitter and base terminals, and the filter is located between the base and collector terminals. The emitter and base are used to supply an operating voltage to the QWIP. The filter is used to accept photoelectrons of certain energies into the collector and rejects the dark electrons from other energies. The rejected electrons then drain through the base terminal. By accepting only electrons at particular energies, the filter reduces the dark current and increases the photocurrent-to-dark current ratio at the collector. Consequently, both the operating temperature and the sensitivity of the detector can be increased. In this project, we model the detector characteristics and the potential performance enhancements, and fabricate small format (5×8) IHET detector arrays to ascertain their advantages.

2. Approach

IHETs in discrete form have been studied in the past (*2*); however, they have not been demonstrated in array formats due to the special contact requirements. Specifically, each IHET requires three external contacts for detector operation, while the usual QWIPs need only two. The existing readout integrated circuits (ROICs) were designed for two-terminal detectors, in which there is only one individual top contact per pixel. A unique array architecture has to be devised for the IHETs if one is to use the existing ROICs. In this work, we propose an architecture that will require only one individual contact for each IHET, and thus, is more compatible with the existing ROICs. In this array format, the collector of the IHET is contacted individually while the emitter and the base are both common to all pixels. It will require the active QWIP layers of all pixels in an array column be joined together. This is feasible only if the current in each pixel is flowing strictly perpendicular to the layers. In principle, this will be the case because the electric field between the emitter and the base is perpendicular to the layers. It is prudent, however, to measure any lateral diffusion of carriers into the neighboring pixels, thus blurring an optical image. The purpose of this project is to determine the electrical cross-talk among different pixels.

3. Results

3.1 Numerical Modeling

Before the experimental effort, it is useful to estimate the expected improvements. In QWIPs, I_d is dominated by the thermally assisted tunneling (TAT) current. The TAT current originates from thermal excitation of the ground state electrons to yield a large in-plane energy, E_{in}. Upon a scattering process, this large E_{in} is transformed into a large E_z perpendicular to the quantum wells (QWs), with which a larger tunneling probability, γ, results. Consequently, the TAT current is given by

$$J_{TAT}(V,T) = \int_{E_1}^{\infty} e\, n_{TAT}(E,V,T)\, v(V)\, dE,$$

where

$$\begin{aligned} n_{TAT}(E,T,V) &= g_{3D}\, f(E,T)\gamma(E,V) \\ &= \frac{m^*}{\pi\hbar^2 L} \frac{\gamma(E,V)}{1+\exp\left(\dfrac{E-E_F-E_1}{kT}\right)}, \end{aligned} \tag{1}$$

is the effective three-dimensional electron density per meV, and f (E) is the Fermi function. Equation 1 satisfactorily explains the observed dark current, such as that of detectors A and B shown in figure 1(a). The only fitting parameter in this plot is the low field electron mobility, μ.

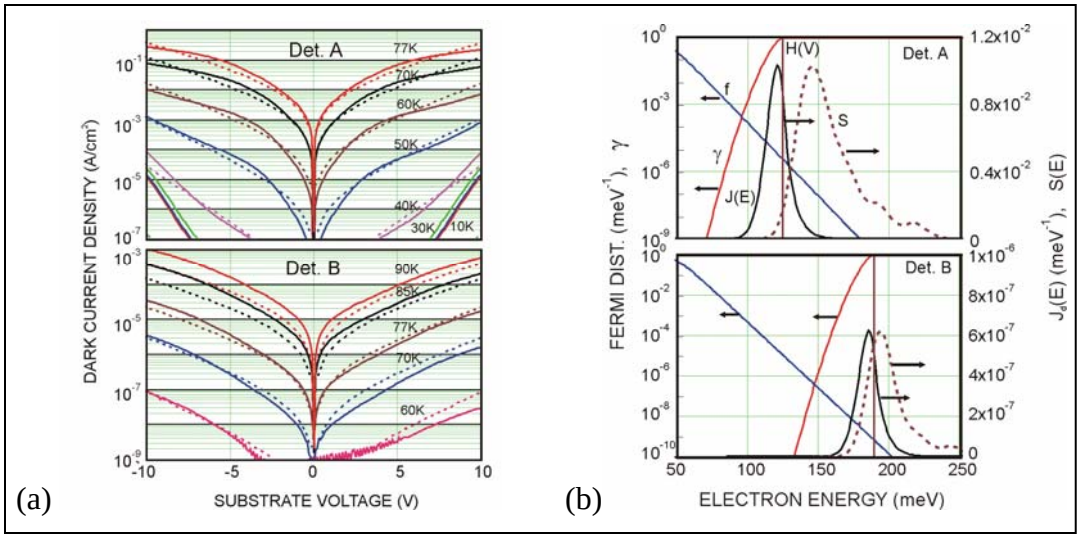

Figure 1. (a) The measured (solid curves) and the fitted (dashed curves) dark currents under different bias and temperatures. Detector A has the nominal $In_yGa_{1-y}As/Al_xGa_{1-x}As$ QW parameters (x, y, well width W, barrier width B) = (0.12, 0.1, 50 Å, 700 Å) and B has (0.21, 0.1, 50, 700). The fitted μ = 400 cm^2/Vs for A and 120 cm^2/Vs for B. (b) The corresponding f(E), γ(E), J(E) ≡ $en_{TAT}(E)v$, and S(E) at 77 K and 80 mV/period.

To obtain additional insights into the energies of the carriers, we plot the functions f(E) and γ(E) at temperature T = 77 K and voltage V = 80 mV per QW period in figure 1(b). Their product has a maximum just below the QW barrier height, H(V). The TAT current is, therefore, conducting just below the barriers, with only a small high energy tail above H(V). Figure 1(b) also shows the energy distribution of the photoelectrons, which is determined by the absorption spectra, S(E), of the detectors. At 80 mV, the photoelectron peak and dark current peak are well separated in energy, especially in detector A.

3.2 Concept of Infrared Hot-Electron Transistors

Since the dark current is conducting below H and the photocurrent is conducting above H, the two groups of electrons can be separated by an energy selective filter as depicted in figure 2. By attaching an additional barrier at one end of the QWIP (the base), one can regulate the passage of the electrons into a new collector terminal, C, according to their energies. With an appropriate collector bias, V_C, one can maximize the photocurrent-to-dark current ratio.

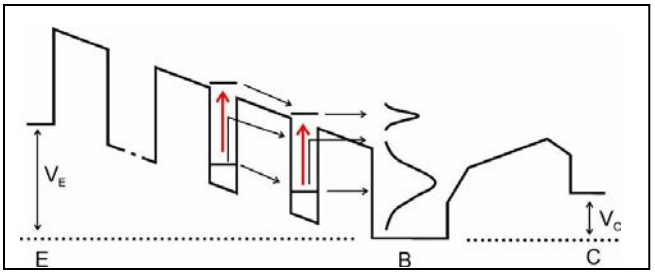

Figure 2. The IHET structure with a thick barrier near the collector C as a high pass filter, showing the higher energy photoelectrons created by optical transition (red arrows) is accepted into the collector while the lower energy TAT current is rejected into the base.

The IHET structure used in the present project is shown in figure 3. It is designed to have a 9.2 μm wavelength cutoff. The calculated dark current transfer ratio, α_d, from the emitter to the collector is shown in figure 4(a). The value of α_d is the fraction of dark electrons with energy above $H(V_E)$ that will not be filtered out by the filter barrier. This fraction of electrons is dependent on both V_E and T. Similarly, the fraction of photoelectrons that has energy above $H(V_E)$ can be calculated from the absorption spectrum and the corresponding photocurrent transfer ratio, α_p, is shown in figure 4(b). Its value depends on the emitter voltage only. After the preferential current filtering, the fraction of photocurrent, I_p, versus the dark current, I_d, in the total collector current, I_C, is increased, which strengthens the signal-to-noise (S/N) ratio. Numerically, the photocurrent-to-dark current ratio measured at the emitter, $r_E \equiv (I_p/I_d)_E$, and that measured at the collector, r_C, is related by $r_C = (\alpha_p/\alpha_d)r_E$. Figure 4(c) shows the value of α_p/α_d at different V and T. For example, at –8 V and 80 K, α_p/α_d is expected to be 5, and therefore, the S/N ratio will improve by the same factor by using the IHET structure.

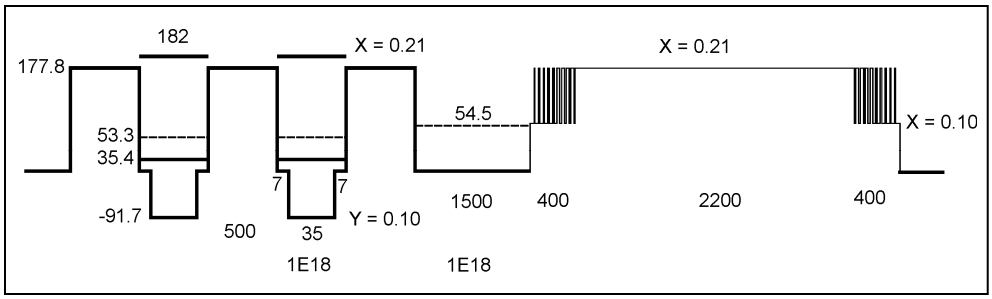

Figure 3. The band diagram and the structural parameters of the present IHET design.

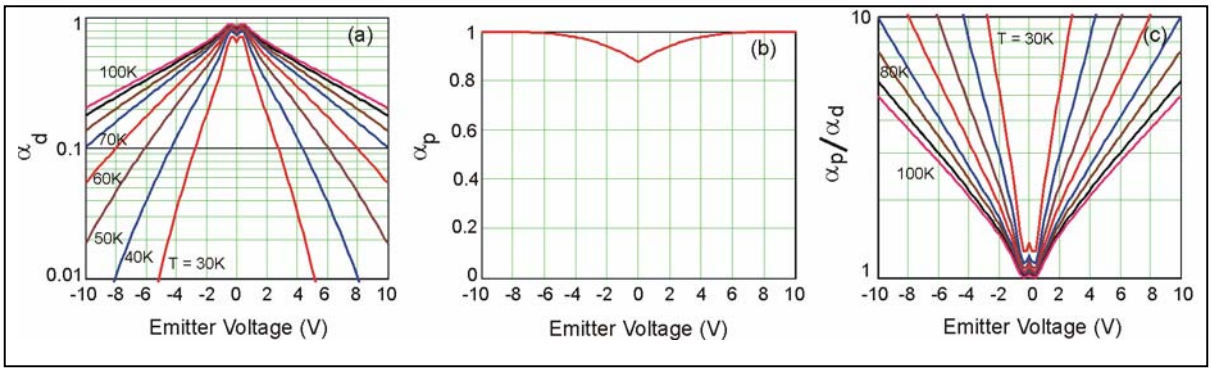

Figure 4. (a) The calculated dark current transfer ratio, (b) the photocurrent transfer ratio, and (c) the photocurrent-to-dark current improvement factor, α_p/α_d, upon energy filtering.

3.3 Array Processing

The main objective for this research is to investigate the common base configuration. This approach is to eliminate the need to have two external contacts for each detector, one for the base and another for the collector. Figure 5(a) shows the mask layout of a 5×8 IHET array. The bottom row is the emitter layer contact common to all pixels. The adjacent row and the top row are the base contacts common to individual detector columns. The center five rows are individual detector collector contacts. To properly operate each array column, a negative V_E is applied to emitter contact, a ground contact is connected to the two base contacts, and a small voltage is applied to individual collector contacts. Figure 5(b) shows the cross section on an array column. To realize this detector architecture, chemical etching was used to divide the wafer into array columns. Precision shallow plasma etching was then used to reach down to the base layer and divides the array into rows. Another deep plasma etching was used to separate the emitter from the base in the same column as shown in figure 5(b). Shallow ohmic contacts consisting of 15 nm palladium (Pd), 20 nm germanium (Ge), and 200 nm gold (Au) were deposited on all contacts and were alloyed at 425 °C for 100 s. Finally, 200 nm magnesium fluoride (MgF_2), 10 nm chromium (Cr), and 200 nm Au were deposited on the detector sidewalls as optical reflectors. The arrays were diced and polished with a 45° facet for optical coupling. For array testing, a row of detectors were wire bonded and mounted in an optical dewar. Figure 6 shows the processed IHET arrays and unit cells.

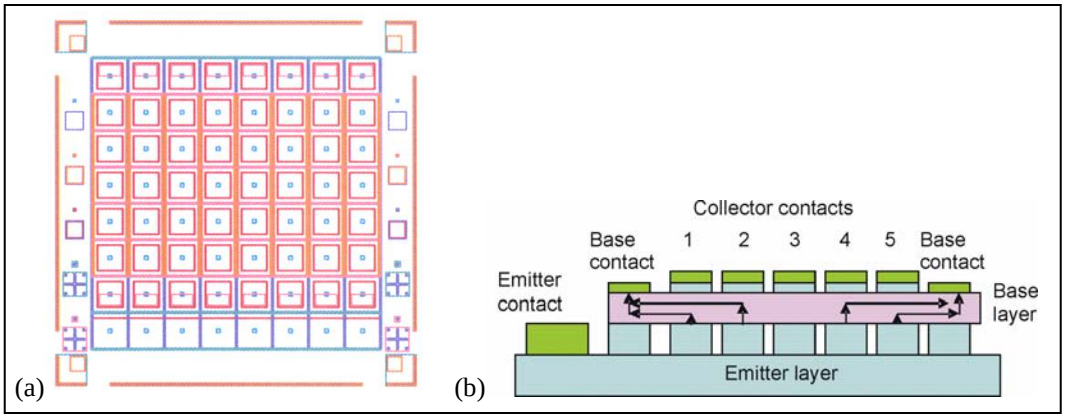

Figure 5. (a) The mask layout of the IHET array and (b) the cross section of an array column.

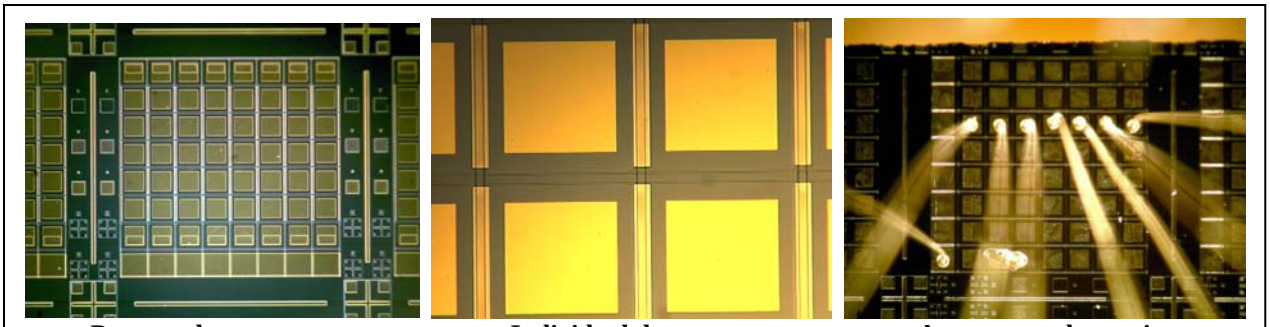

Figure 6. Processed IHET arrays.

3.4 Experimental Results

Emitter and collector spectral responses from a test array were measured at different V_E and V_C. The results are shown in figure 7. The emitter responsivity, which represents the response from the QWIP, matches the designed spectrum, confirming the QWIP material growth. However, the collector response, R_C, is about one order of magnitude less than the emitter response, R_E, showing that there is a large photocurrent reduction. Extrapolating the trend of R_C versus V_C, it would require a large V_C of 2.5 V to capture ~80% of the photoelectrons. This large V_C requirement is attributed to the finite background doping in the filter barrier that raises the filter barrier height.

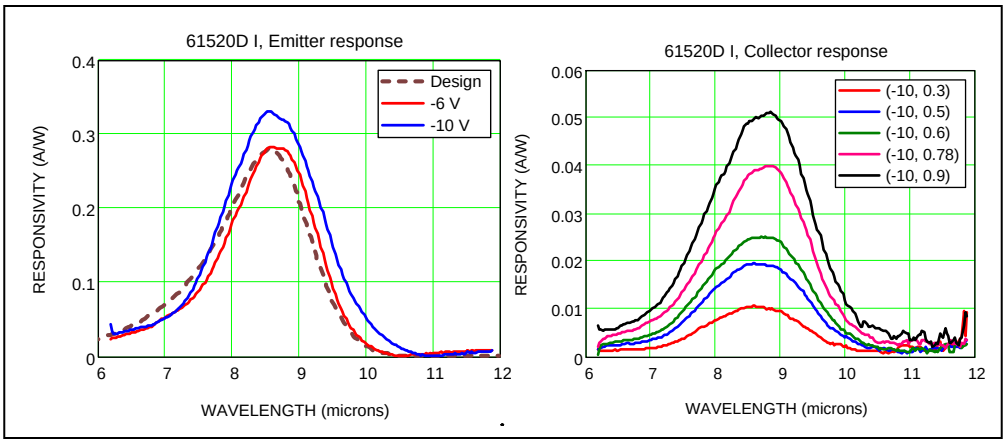

Figure 7. Emitter spectral response at V_E = –6 and –10 V (left panel) and collector response at V_E = –10 V and V_C = 0.3–0.9 V (right panel).

The emitter and collector dark current data are shown in figure 8(a). The overlapping solid curves on top are the emitter current density, J_E, at different V_C and different number of collectors being connected. This constant J_E indicates good electrical isolation between the QWIP stage and the collector stage. The dashed curves are the collector current densities, J_C. The large reduction of dark current is also consistent with a higher filter barrier. The top two overlapping dash curves are J_C from a single detector with the other collector contacts connected to each other (dashed pink) or disconnected from the circuit (dashed brown). This excellent overlap indicates no detector cross-talk existed in this array. This important result validates that no electrical signal will transfer from one detector to the next through the common base contact. The black, blue, and red dash curves are J_C at V_C = 0.4, 0.3, and 0.2 V, respectively. Similarly, the photocurrent density is measured and is shown in figure 8(b).

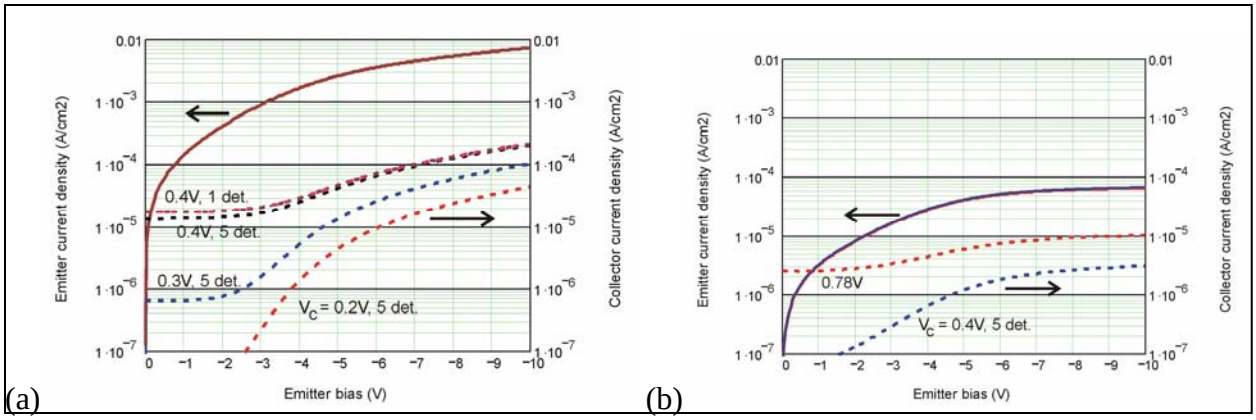

Figure 8. (a) Dark current density and (b) photocurrent density vs. V_E at 77 K.

Figure 9(a) compares the dark current transfer ratio α_d at 77 K (black curves) and the photocurrent transfer ratio α_p (red curves) at V_C = 0.4 V. It is apparent that $\alpha_p > \alpha_d$ in the entire bias range. The largest α_p/α_d is 6 at V_E = 1.2 V as shown in figure 9(b).

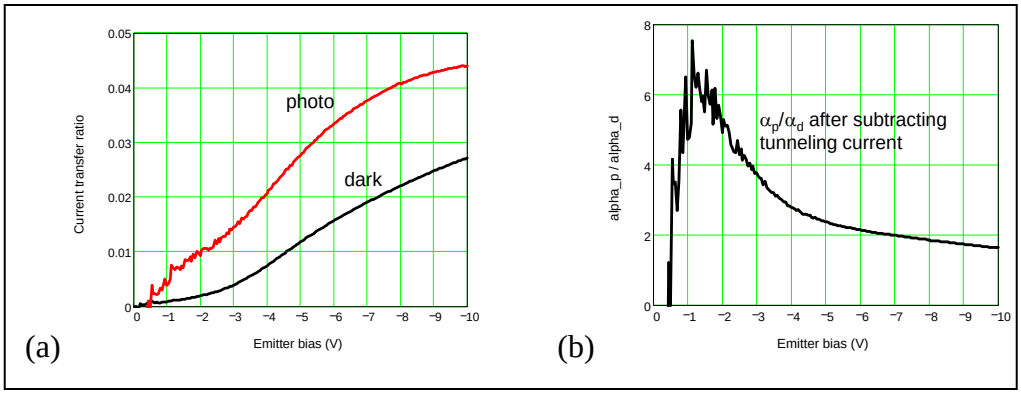

Figure 9. Emitter to collector current transfer ratio curves vs. emitter bias at V_C = 0.4V.

4. Conclusions

In this study, we investigated a 5×8 corrugated IHET array with a common base configuration. The IHET structure improved the photocurrent-to-dark current ratio by a maximum factor of six, and hence, it will improve the array S/N ratio by the same factor. The study also showed that there is no electrical cross-talk among individual detectors, even though they share the same emitter and base contacts. Thus, it paves the way to high density sensitive focal plane arrays.

5. References

1. Choi, K. K.; Dutta, M.; Newman, P. G.; Saunders, M. L.; Iafrate, G. J. 10 micron infrared hot electron transistors. *Appl. Phys. Lett.* **1990**, *57*, 1348.

2. Lee, C. Y.; Choi, K. K.; Leavitt, R. P.; Eastman, L. F. Infrared hot-electron transistor with a narrow bandpass filter for high temperature operation. *Appl. Phys. Lett.* **1995**, *66*, 90.

6. Transitions

Preliminary results have been presented in a 2008 Society of Photo-Optical Instrumentation Engineers (SPIE) meeting:

Choi, K. K.; Forrai, D. P.; Endres, D.; Sun, J.; Pinsukanjana, P.; Devitt, J. W. C-QWIP focal plane array development, *Proceedings of SPIE,* San Diego, CA, 10–14 August 2008,Vol. 7082.

Acronyms

Au	gold
Cr	chromium
Ge	germanium
IHET	infrared hot-electron transistor
MgF_2	magnesium fluoride
Pd	palladium
QWIP	quantum well infrared photodetector
QWs	quantum wells
ROICs	readout integrated circuits
S/N	signal-to-noise
TAT	thermally assisted tunneling

Copies	Organization
1 (PDF only)	DEFENSE TECHNICAL INFORMATION CTR DTIC OCA 8725 JOHN J KINGMAN RD STE 0944 FORT BELVOIR VA 22060-6218
1	DIRECTOR US ARMY RESEARCH LAB IMNE ALC HR 2800 POWDER MILL RD ADELPHI MD 20783-1197
1	DIRECTOR US ARMY RESEARCH LAB AMSRD ARL CI OK TL 2800 POWDER MILL RD ADELPHI MD 20783-1197
1	DIRECTOR US ARMY RESEARCH LAB AMSRD ARL CI OK PE 2800 POWDER MILL RD ADELPHI MD 20783-1197
12	US ARMY RESEARCH LAB AMSRL ARL SE SG R FU AMSRD ARL SE EI W BECK D BEEKMAN K-K CHOI P FOLKES J LITTLE K OLVER F SEMENDY J SUN S SVENSSON P UPPAL P WIJEWARNASURIYA 2800 POWDER MILL RD ADELPHI MD 20783-1197

ABERDEEN PROVING GROUND

1	DIR USARL AMSRD ARL CI OK TP (BLDG 4600)

TOTAL 17 (1 ELEC, 4 CDs, 12 HCs)

INTENTIONALLY LEFT BLANK.